*Proceedings of "Applications of Physics in Mechanical and Material Engineering" (APMME 2023)*

# Changes in the Surroundings of the Central Iron Atom in Amorphous Alloys

P. Pietrusiewicz*

*Department of Physics, Faculty of Production Engineering and Materials Technology, Czestochowa University of Technology, al. Armii Krajowej 19, 42-200 Częstochowa, Poland*

Doi: 10.12693/APhysPolA.144.383 *e-mail: pawel.pietrusiewicz@pcz.pl

Amorphous alloys are still a challenge for science when it comes to an accurate description of their structure and magnetic properties. There are many techniques for studying the structure, however, the direct observation of the amorphous structure does not bring much to the description of the phenomena occurring in them. In the case of ferromagnetic amorphous alloys, their properties can be studied based on the analysis of transmission Mössbauer spectra and the hyperfine field induction distributions obtained on their basis. The work investigated the influence of changing the surroundings of the central iron atom on the magnetic properties of a soft magnetic amorphous alloy. Samples after solidification and after isothermal annealing at a temperature below the crystallization temperature were tested.

topics: Mössbauer spectroscopy, amorphous materials, soft magnetic materials

## 1. Introduction

Amorphous iron-based materials are also called metallic glasses (MG). They offer many technical applications and are characterized by very good mechanical and soft magnetic properties. Soft magnetic materials are characterized by a low coercive field of less than 1000 A/m. However, materials with an amorphous structure are characterized by the lack of boundary grains in their structure, unlike materials with a crystalline structure of the same chemical composition. Metallic glasses have been studied for many decades [1–4] in various respects, i.e., magnetic and mechanical properties, structural system, and thermal stability, using various types of measurement methods, including X-ray diffraction (XRD), differential scanning calorimetry (DSC), scanning electron microscopy (SEM), Mössbauer spectrometry, etc. [3–7]. It is also known that the properties of amorphous alloys can be improved by applying appropriate annealing at temperatures below the crystallization temperature. There are many items in the literature regarding the annealing of amorphous materials below the crystallization temperature [8–12]. However, such optimization led to the formation of a nanocrystalline phase, usually $\alpha$-Fe phase grains embedded in an amorphous matrix.

In the work of T. Naohara [13], it was shown that the optimization process can proceed without the formation of grains of the $\alpha$-Fe nanocrystalline phase and lead to a reduction of internal stresses in the free volume areas and a change in the immediate surroundings of Fe atoms, which may lead to the stabilization of magnetic properties. Using Mössbauer spectroscopy, changes in the environment of the closest neighbors of Fe atoms can be assessed [14]. Mössbauer spectroscopy is a powerful tool used to study local magnetic properties and chemical and crystallographic disturbances. Based on the analysis of Mössbauer spectra, the influence of changing the surroundings of the central iron atom on the magnetic properties of the soft magnetic amorphous $(Fe_{61}Co_{10}Y_8W_1B_{20})Pt_1$ alloy was investigated. Samples were tested after solidification and after isothermal annealing at a temperature below the crystallization temperature.

## 2. Experimental procedure

The research material with atomic composition $(Fe_{61}Co_{10}Y_8W_1B_{20})Pt_1$ was melted in an arc furnace in a protective atmosphere of inert gas (Ar). High-purity elements were used to produce the alloys, namely Fe — 99.98%, Co — 99.95%, Y — 99.9%, W — 99.95%, B — 99.5%, and Pt — 99.99%. Amorphous ribbons were produced using the melt-spinning method with a rotational speed of a copper wheel of 35 m/s. The produced ribbons, 5 mm wide and 35 mm thick, were annealed at three temperatures: at 600 K for 1 h, at 700 K for 1 h, and at 800 K for 1 h. After each annealing stage, the ribbon samples were tested using a Mössbauer transmission spectrometer with a $^{57}$Co source in an Rh

TABLE I

Results of analysis of Mössbauer spectra, where $IS$ — isomer shift, $B_{hf}$ — hyperfine magnetic field, $D_{am}$ — standard deviation, $Q_{UA}$ — quadrupole splitting, $A23$ — relative line intensity ratio.

| | $IS$ [mm/s] | $B_{hf}$ [T] | $D_{am}$ [T] | $Q_{UA}$ [mm/s] | $A23$ |
|---|---|---|---|---|---|
| As-cast | −0.091(2) | 19.685 | 5.357 | −0.0206(8) | 2.396(6) |
| 600 K | −0.091(2) | 19.646 | 5.349 | −0.0224(1) | 2.599(9) |
| 700 K | −0.092(1) | 19.669 | 5.353 | −0.021(2) | 2.451(6) |
| 800 K | −0.092(6) | 20.092 | 5.417 | −0.0207(9) | 2.557(6) |

matrix with an activity of 100 mCi. The spectrometer speed calibration was performed on $\alpha$-Fe foil with a purity of 4 N, the hyperfine field of which is $B_{hf} = 33.1$ T at room temperature. Mössbauer spectra were fitted using NORMOS software.

### 3. Results and discussion

Experimental Mössbauer spectra recorded for samples of the $(Fe_{61}Co_{10}Y_8W_1B_{20})Pt_1$ alloy are shown in Fig. 1. The spectra of each sample were recorded in the same transmission geometry and with similar measurement times. Each of the measured spectra was decomposed into a set of 34 elementary Zeeman sextets and fitted using the least squares method. Each spectral line was expressed using hyperfine parameters such as hyperfine magnetic field ($B_{hf}$), isomeric shift ($IS$), and quadrupole splitting ($Q_{UA}$), and the ratio of the intensities of lines 2 and 5 to lines 3 and 4 of the Mössbauer spectrum was determined. Quadrupole splitting was used for fitting due to the possible noncubic symmetry of atomic configurations around $^{57}$Fe [15]. All fitting parameters of the Mössbauer spectra are listed in Table I.

Based on the measured Mössbauer spectra, it can be concluded that the tested materials are ferromagnetics with an amorphous structure. The wide asymmetric lines of the Mössbauer spectra correspond to different surroundings of Fe atoms.

Different environments in the nuclei of $^{57}$Fe atoms in the tested samples confirm the bimodal distributions of the magnetic hyperfine fields $P(B)$ shown in Fig. 2 [3, 16]. The distributions for all tested samples, both after solidification and after annealing at temperatures of 600, 700, and 800 K, are similar and consist of two clearly separated peaks: low and high field. It can be seen that the broad peak with the maximum of the average hyperfine field ($B_{hf}$) for the sample in the after-solidification state and for samples annealed successively at temperatures of 600 and 700 K occurs at a field induction of $\sim$ 21 T, while for the sample annealed at 800 K, it occurs at field induction $\sim$ 22 T.

However, the low-field component described by the first peak in the hyperfine field distributions has the maximum value of the average hyperfine field induction at an induction field between 10–11 T.

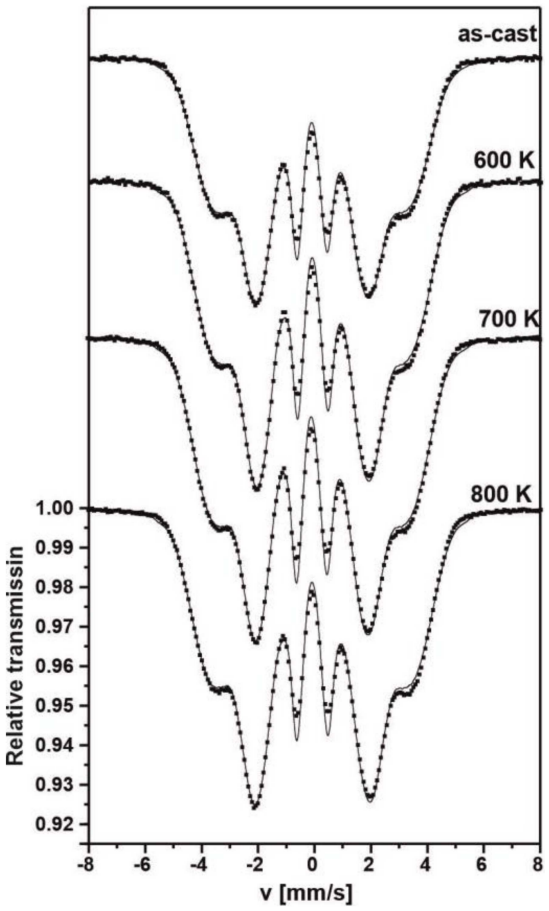


Fig. 1. Transmission Mössbauer spectra for the alloy sample after solidification and after annealing at three temperatures.

In [17], it was postulated that the low-field component corresponds to the presence of Y atoms in near-neighborhood to Fe atoms. This proves that Y in the first coordination zone of Fe, which results in a significant reduction of the hyperfine field [17].

The average hyperfine fields ($B_{hf}$) remain almost constant for the alloy samples after solidification and annealing at temperatures of 600 and 700 K. This can be related to the stable short-range order in the local surroundings of Fe atoms. Only annealing at a temperature of 800 K resulted in an increase in the average hyperfine field ($B_{hf}$) to the

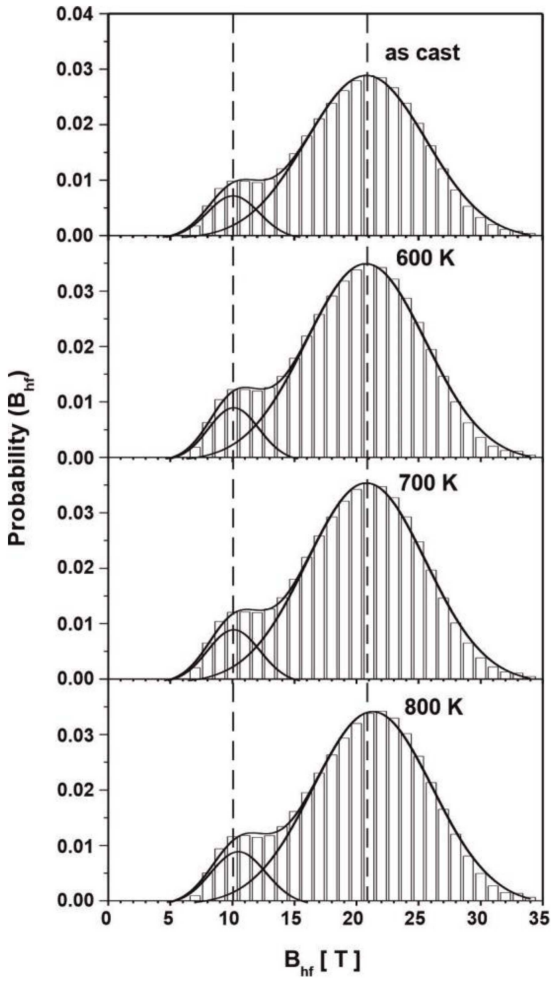


Fig. 2. Distributions of hyperfine fields for samples of the $(Fe_{61}Co_{10}Y_8W_1B_{20})Pt_1$ alloy after solidification and annealing at temperatures of 600, 700, and 800 K.

value of 20.09 T and an increase in the value of decomposition dispersion ($D_{am}$), which is related to the relaxation of the amorphous phase within the free volumes, which reduces the average distance between Fe–Fe atoms.

The surroundings of $^{57}$Fe nuclei in the structure of amorphous materials are also characterized by average values of isomeric shifts ($IS$). The magnetic anisotropy of these shifts can be characterized by the parameter $A23$, i.e., the ratio of lines 2 and 5 of the split Zeeman sextet to lines 3 and 4. The intensity of these lines in the spectrum is determined by the angle $\theta$ between the direction of magnetization of the sample and the radiation $\gamma$. In the absence of any stresses in the sample, the magnetic moments can be expected to be aligned along the plane of the tape due to the anisotropy of the shape. In this case, parameter $A23 = 4$. However, if the magnetic structure in the sample is disordered, the intensity parameter $A23 = 2$. By analyzing the $A23$ parameter, the magnetic texture of the tested samples can be assessed [1, 3].

The values of the isomeric shift ($IS$) and the $A23$ parameter for samples after solidification and annealing at temperatures of 600, 700, and 800 K for 1 h are listed in Table I. It can be seen that annealing did not affect the isomeric shift ($IS$) value, which may indicate that there are no major deviations in the chemical order of the tested materials. Nevertheless, the value of the $A23$ parameter increased after the first stage of annealing at 600 K for 1 h ($A23 = 2.599$), then decreased slightly after annealing at 700 K ($A23 = 2.451$), and increased again after annealing at 800 K ($A23 = 2.557$). This indicates that the annealing process caused the orientation of the magnetic spins to become orderly towards the plane of the tape.

## 4. Conclusions

To sum up, it can be said that the tested material is a ferromagnetic with an amorphous structure. Mössbauer spectra and the corresponding hyperfine field distributions $P(B_{hf})$ for samples after solidification and annealing at temperatures of 600, 700, and 800 K for 1 h do not show significant differences. However, the parameters of individual spectra for the sample heated at 800 K for 1 h show a change in parameters, i.e., the average hyperfine field ($B_{hf}$) and an increase in the dispersion of the distribution ($D_{am}$), which proves the relaxation of the amorphous phase within the free volumes.

The tested alloy $(Fe_{61}Co_{10}Y_8W_1B_{20})Pt_1$ in the form of a ribbon showed very high thermal stability in a wide temperature range.

## References

[1] E. Kuzmann, S. Stichleutner, A. Sápi, L.K. Varga, K. Havancsák, V. Skuratov, Z. Homonnay, A. Vértes, *Hyperfine Interact.* **207**, 73 (2012).

[2] A.K. Bhatnagar, *Hyperfine Interact.* **25**, 637 (1985).

[3] N. Amini, M. Miglierini, J. Dekan, *AIP Conf. Proc.* **1781**, 020020 (2016).

[4] S.L. Panahi, P. Ramasamy, F. Masdeu, M. Stoica, J. Torrens-Serra, P. Bruna, *Metals* **11**, 1293 (2021).

[5] X. Li, K. Zhang, C. Wang, W. Han, G. Wang, *J. Mater. Sci. Technol.* **23**, 253 (2007).

[6] E. Jakubczyk, *Mater. Sci.-Pol.* **24**, 4 (2006).

[7] M.E. McHenry, D.E. Laughlin, in: *Physical Metallurgy*, 5th Ed., Elsevier, 2014 p. 1881.

[8] Y. Yoshizawa, S. Oguma, K. Yamauchi, *J. Appl. Phys. B*, **64** 6044 (1988).

[9] A. Makino, T. Hatani, Y. Naitoh, T. Bitoh, A. Inoue, *IEEE Trans. Magn.* **33**, 3793 (1997).

[10] X. Liang, T. Kulik, J. Ferenc, B. Xu, *J. Magn. Magn. Mater.* **308**, 227 (2007).

[11] J. Zbroszczyk, A. Młyńczyk, J. Olszewski, W. Ciurzyńska, M. Hasiak, R. Kolano, J. Lelątko, *J. Magn. Magn. Mater.* **304**, e727 (2006).

[12] R. Hasegawa, *J. Magn. Magn. Mater.* **304**, 187 (2006).

[13] T. Naohara, *Philos. Mag. Lett.* **78**, 229 (1998).

[14] Nan Zhang, Gang Li, Xin Wang, Tao Liu, Jianliang Xie, *J. Alloy. Compd.* **672**, 176 (2016).

[15] J. Kansy, A. Hanc, J. Rasek, G. Haneczok, L. Pająk, Z. Stokłosa, P. Kwapuliński, *Acta Phys. Pol. A* **119**, 41 (2011).

[16] M. Nabiałek, P. Pietrusiewicz, K. Błoch, *J. Alloy. Compd.* **628**, 424 (2015).

[17] P. Gupta, A. Gupta, A. Shukla, Tapas Ganguli, A.K. Sinha, G. Principi, A. Maddalena, *J. Appl. Phys.* **110** 033537 (2011).